CREATING A GLOBAL GEOLOGICAL MAP OF MERCURY WITH MESSENGER DATASETS. Mallory J. Kinczyk[1], Paul K. Byrne[1], Louise. M. Prockter[2], Brett W. Denevi[3], Lillian R. Ostrach[4], James A. Skinner[4], Debra L. Buczkowski[3], Brian M. Hynek[5]. [1]Planetary Research Group, North Carolina State University, Raleigh, NC 27695. [2]The Lunar and Planetary Institute, Houston, TX 77058. [3]The Johns Hopkins University Applied Physics Laboratory, Laurel, MD 20723. [4]U.S. Geological Survey, Astrogeology Science Center, 2255 N. Gemini Dr., Flagstaff, AZ 86001. [5]University of Colorado, Boulder, CO 80303, USA.

Introduction: The MErcury Surface, Space ENvironment, GEochemistry, and Ranging (MESSENGER) spacecraft orbited Mercury from 2011 to 2015 and imaged the planet in its entirety. A global monochrome image mosaic was released to the Planetary Data System (PDS) in 2016 at a resolution of ~250 m/pixel [1], allowing for rigorous geomorphological mapping on a global scale. This vastly improved data product forms the basis for the first global geological map of Mercury [2] —which will facilitate the comparison of units distributed discontinuously across Mercury's surface, enabling the development of the first global stratigraphic column and providing a guiding basis for future investigations involving the planet's geological history.

Map Status: The map has been prepared for publication at 1:15M scale and will be submitted to a peer-reviewed journal for publication. However, the standards for maps published following USGS guidelines afford detailed community feedback and result in a product that will provide a more robust basis for future mappers and missions. As a result, a proposal was submitted to and funded through the PDART program to publish the map as a USGS Scientific Investigations Map (SIM) series product.

Geomorphological units for the current map were delineated on the basis of texture, color, and topographical relief. These include impact craters, intercrater plains [3], smooth plains [4], and ejecta facies of several large impact basins [5-7], as well as linear/point features such as tectonic landforms [8], hollows [9], and pyroclastic vents [10]. Efforts going forward for the SIM will be focused on improving the state of mapped unit boundaries based on data products that are currently being finalized and will be publicly available in a final MESSENGER PDS data release in the coming months, These data will also be used to enhance the map with additional delineated units as warranted.

Mercury's Intercrater Plains: At present, the intercrater plains unit is the most extensive mapped unit on Mercury's surface. It comprises plains materials that lie between large craters and basins and contains a high spatial density of small superposed craters 5–15 km in diameter [3]. The origin of intercrater plains has been disputed, with proposed mechanisms including effusive volcanism and impact melt pools originating from ancient large impact events [11,12]. Assessing spatial color variation within the intercrater plains could further our understanding of the spatial and temporal differences within this large region on Mercury's surface. Previously, artifacts from temporal variation of the Wide-Angle Camera responsivity were as large as or larger than Mercury's true color variations, preventing reliable comparisons of regional color properties. However, recalibrated data now accurately resolve regional color variations within the intercrater plains [12].

Denevi et al. [12] identified an isolated area of intercrater plains with different color properties than the surrounding regions, centered at ~10° N, 270° E (**Fig. 1**). Throughout this region, the intercrater plains have moderate reflectance and most impact craters with distinct ejecta deposits expose high-reflectance red material (HRM), defined by a steeper spectral slope and elevated reflectance relative to Mercury's mean. HRM is spectrally equivalent to smooth plains deposits [13], and examples of such material exposed by impact craters [14] were thought to represent older generations of buried volcanic plains. The margins of this area (shown in enhanced color in **Fig. 1a**) mark a transition to more frequent exposures of low-reflectance material (LRM) within craters and lower overall surface reflectance. This is one of several regions of observed color variations within the intercrater plains.

As part of our work to prepare the Mercury global SIM, we will seek to characterize regional changes in color, topographic and compositional differences, and variations in crater degradation and crater size–frequency distributions to identify and distinguish Pre-Tolstojan and Tolstojan intercrater plains. The presently available enhanced color mosaic shows evidence that the intercrater plains are not a morphologically or temporally homogeneous unit. Therefore, identifying, resolving, and including these subdivisions in the Mercury global SIM will provide information critical to future studies of the planet's stratigraphy and early geological history.

Deriving Age Estimates for Major Surface Units: Relative and absolute model ages will be determined by evaluating stratigraphic relationships and crater measurements (areal densities and crater size-frequency distributions) for units delineated during this work as well as reevaluating published crater size-frequency distributions for previously delineated units.

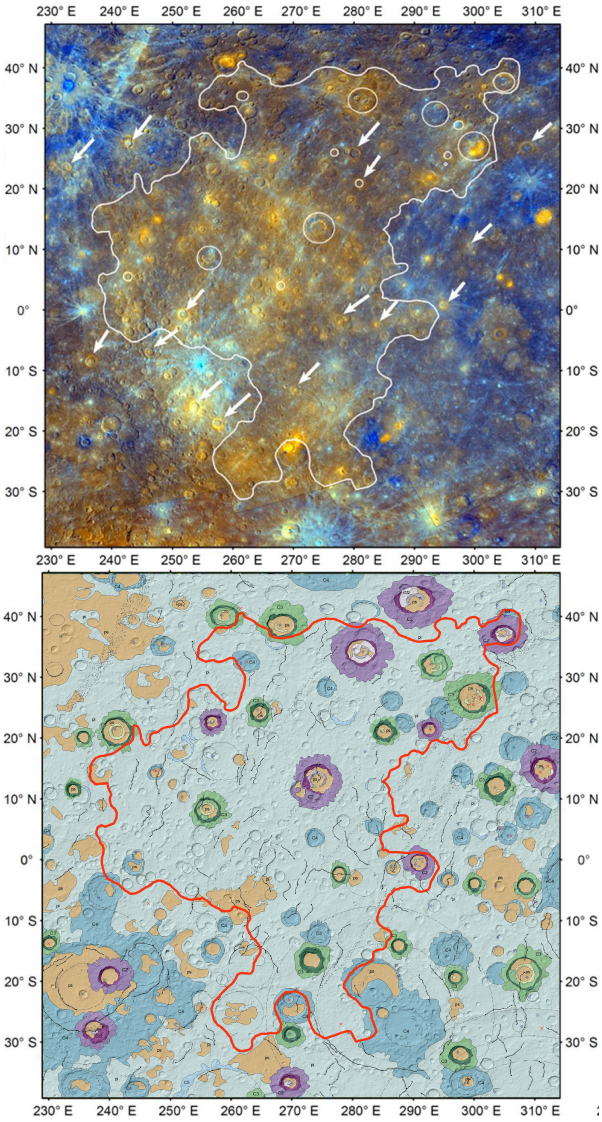

Figure 1. (a) Region of intercrater plains containing prominent areas of HRM in the enhanced color mosaic. (b) Current geological map of Mercury (intercrater plains shown in light blue) with outline of possible addition of high-reflectance intercrater plains unit in red.

Impact craters ≥8 km in diameter will be measured for representative regions of each major mapped surface unit, including possible intercrater plains units, major impact basin-related units (such as the Caloris and Rembrandt units), and select smooth plains units.

By deriving their crater size-frequency distributions, we will place each unit into the current chronostratigraphic system for Mercury (i.e., Pre-Tolstojan, Tolstojan, Calorian, Mansurian, and Kuiperian [15]). Representative sections of each unit will be selected on the basis of a spatial randomness analysis [16,17]. Absolute model ages for mapped units will be derived with two modern chronologies for Mercury [18–20].

Revising Existing Linear and Point Features: As is the case for the other data sets we will compile in the Mercury global SIM, the existing maps of shortening and extensional structures will be refined with the updated control network and improved viewing geometries of the latest MDIS basemaps [1] at a scale of 1:5M (to be published at 1:15M scale). We will in general follow the approach used in preparing the existing map of including only those shortening structures ≥100 km in length, but in places it may be appropriate (e.g., for areas of shortening deformation but where no structures ≥100 km long occur) to incorporate shorter landforms. For extensional structures, we will include examples ≥50 km in length (which represents a balance between map completeness and representing structural complexity), but will again map shorter examples at given locations if their exclusion on the map would otherwise imply that no extensional deformation resolvable at 1:5M occurs there.

We will also incorporate those landforms on Mercury too small to map discretely at the 1:5M scale as point features, e.g., hollows and pyroclastic vents and their associated deposits. In the current map, these features were based upon global surveys conducted prior to the availability of the revised global control network [9,10]. These features will be reevaluated to ensure their locations are updated.

These tasks will improve the state of the current geological map and will lead to a product that will be consistent in scientific utility with other USGS SIM products.

References: [1] Chabot, N.L. et al. (2016) *LPS, 47,* #1256. [2] Prockter, L.M. et al. (2016) *LPS, 27,* #1245. [3] Whitten, J.L. et al. (2014) *Icarus, 241,* 97–113. [4] Denevi, B.W. et al. (2013) *J. Geophys. Res. Planet, 118,* 891–907. [5] Hynek, B.M. et al. (2016) *LPS, 47,* #2312. [6] Buczkowski, D.L. et al. (2015) *LPS, 46,* #2287. [7] Prockter, L.M. et al. (2009) *LPS, 40,* #1758. [8] Byrne, P.K. et al. (2014) *Nature Geosci., 7,* 301–307. [9] Blewett, D.T. et al. (2013) *Science, 333,* 1856-1859. [10] Thomas, R.J. et al. (2014) *J. Geophys. Res. Planets, 119,* 2239–2254. [11] Wilhelms D. E. (1976) *Icarus, 28,* 551–558. [12] Denevi, B.W. et al. (2016) *LPS, 47,* #1624. [13] Head, J.W. et al. (2011) *Science, 333,* 1853–1856. [14] Ernst, C.M. et al. (2010) *Icarus, 209,* 210-223. [15] Spudis, P.D. and Guest, J.E. (1988) in *Mercury, U. Ariz. Press,* 118–164. [16] Michael, G.G. et al. (2012) *Icarus, 218,* 169-177. [17] Platz, T.G. et al. (2013) *Icarus, 225,* 806-827. [18] Marchi, S.A., et al. (2009) *Astron. J., 137,* 4936-4948. [19] Marchi, S.A., et al. (2013) *Nature, 499,* 59-61. [20] Le Feuvre, M. & Wieczorek, M.A. (2011) *Icarus, 214,* 1–20.